communications biology

A Nature Portfolio journal

Article

https://doi.org/10.1038/s42003-025-08943-7

Lignocellulose degradation capabilities and distribution of antibiotic resistance genes and virulence factors in *Clostridium* from the gut of giant pandas

Check for updates

Wenwen Deng [1,2,4], Caiwu Li[2,4], Yan Huang[2], Chengxi Liu[1], Rengui Li[2], Ti Li[2], Daifu Wu[2], Yongguo He[2], Desheng Li[2], Shengzhi Yang [3,5] ✉, Likou Zou [1,5] ✉ & Ke Zhao [1,5] ✉

Clostridium is a vital gut anaerobe in giant pandas (GPs), aiding bamboo digestion and gut homeostasis. The present study optimizes anaerobic culturing to isolate *Clostridium* species from GPs, evaluating their ecological roles in bamboo digestion while assessing associated pathogenic and antibiotic resistance threats. The results show that the enriching samples in liquid media facilitated the isolation of *Clostridium* species. A total of 14 species are obtained, with *C. perfringens*, *C. sardiniense*, and *C. baratii* being most prevalent. 86.30% of strains exhibit lignocellulose-degrading activity, with all *C. butyricum* strains displaying activity for β-glucosidase, xylanase, and manganese peroxidase. Genomic analysis identifies carbohydrate-active enzymes and metabolic pathways involved in lignocellulose degradation, short-chain fatty acid production, and essential amino acid biosynthesis. *C. butyricum* possesses the most hemicellulose- and cellulose-degrading genes. We also identify 19 antibiotic resistance genes (ARGs), predominantly glycopeptide-resistant *van* genes, and 23 virulence factors (VFs) encoded by 408 virulence genes (VGs). Notably, *C. perfringens* harbors the most ARGs and VFs, some of which are flanked by mobile genetic elements, suggesting risks of horizontal gene transfer. Overall, this study describes the dual role of *Clostridium* in GPs, contributing to dietary adaptation while also posing potential hazards due to pathogenic traits and antimicrobial resistance.

The giant panda (GP) (*Ailuropoda melanoleuca*) gastrointestinal tract harbors a complex and diverse gut microbiota, consisting of bacteria, fungi, protozoa, and viruses, that regulates many essential physiological processes and plays a vital role in the health of GPs[1]. Among these microbial constituents, bacterial communities have received special attention due to their predominance and functional significance. In recent years, next-generation sequencing (NGS) technology, including 16S rRNA, metagenomic, and meta-transcriptomes, has enhanced our understanding of the compositional and functional dynamics of the gut microbiota of GPs[2–4]. For example, it is widely recognized that three phyla—Firmicutes, Bacteroidetes, and Proteobacteria—dominate the gut microbiota of captive and wild GPs[3,5]. Additionally, research on the co-evolution between GPs and their gut symbionts demonstrated that the gut microbiome in captive GPs possessed more genes related to multi-drug resistance, whereas the gut microbiome in wild GPs possessed more genes for host genetically specific structures and functions[6].

Numerous metabolic processes in healthy colonocytes involve high-oxygen consumption, which contributes to maintaining an anoxic or anaerobic gut environment, thereby providing a favorable habitat for an abundance of anaerobic bacteria[7,8]. Culture-independent sequencing approaches have identified several anaerobic genera in the gut of GPs, such as *Clostridium*, *Bifidobacterium*, *Terrisporobacter*, and *Veillonella*, with *Clostridium* being the predominant genera[3]. Members of the genus *Clostridium* are Gram-positive, endospore-forming, obligate anaerobes that

[1]College of Resources, Sichuan Agricultural University, Chengdu, Sichuan, China. [2]Key Laboratory of State Forestry and Grassland Administration (SFGA) on Conservation Biology of Rare Animals in the Giant Panda National Park, The China Conservation and Research Center for the Giant Panda (CCRCGP), Chengdu, Sichuan, China. [3]College of Life Science, Sichuan Agricultural University, Ya'an, Sichuan, China. [4]These authors contributed equally: Wenwen Deng, Caiwu Li. [5]These authors jointly supervised this work: Shengzhi Yang, Likou Zou, Ke Zhao. ✉e-mail: sclzysz@qq.com; zoulikou@sicau.edu.cn; zhaoke82@126.com

have been reported to have both positive and negative effects on gut homeostasis and body health via directly or indirectly interacting with the other resident microbial populations, as well as providing fundamental and specific functions, especially in metabolic and immune processes[9,10]. Moreover, *Clostridium* has been shown to exert metabolic effects that positively influence gut inflammation, cancer therapy, and energy metabolism[11]. *Clostridium* colonizes the GP gut during breastfeeding early in infancy and becomes a member of the gut microbiome following weaning onto a bamboo diet[5]. *Clostridium* is understood to aid the adaptation of GPs to a high-fiber diet, as it is an effective lignocellulose degrader[12,13]. However, further studies are needed to determine the prevalence of lignocellulose-degrading *Clostridium* in GPs and if different *Clostridium* species have varying lignocellulose-degrading capabilities.

The genus *Clostridium* also includes opportunistic pathogens that are capable of causing gut diseases, largely dependent on the various types of virulence factors (VFs) produced[14,15]. These pathogens can induce histotoxic infections when toxins enter the bloodstream and damage internal organs[16]. Antibiotic treatments are frequently used to treat these infections, which may result in the storage and transmission of antibiotic resistance genes (ARGs) in the gut microbiota, raising concerns about increasing resistance among *Clostridium* species[17,18]. Current understanding of ARGs and VFs in giant panda gut microbiota primarily stems from metagenomic studies, which revealed that the genus *Clostridium* contributes to the ARG pool, with particular species emerging as dominant reservoirs[6,19]. However, existing studies have primarily focused on comparative analyses of ARG and VF profiles across geographical populations and management conditions (captive, reintroduced, and wild), rather than strain-level characterization[20,21]. Consequently, cultivation-based studies systematically evaluating ARG and VF distribution among different *Clostridium* species remain limited. This gap underscores the need to understand VFs and ARGs distribution within the *Clostridium* genus to develop more effective therapeutic strategies for relevant diseases.

In recent years, the generation of genomic binning has made it possible to reconstruct microbial genomes from shotgun metagenomic sequencing data, which provides insights into the microbial communities and their potential functions at the species level[22,23]. A large number of metagenome-assembled genomes (MAGs) have been recovered from the gut of GPs. These MAGs were comprised of several bacterial strains within the *Clostridium* species, including *C. perfringens*, *C. ventriculi*, *C. paraputrificum*, and *C. neonatale*[4]. However, metagenomic assembly approaches only catch a limited portion of bacterial populations, leaving minority species unidentified. Thus, the majority of MAGs remain unclassified at the species level[24]. Given that a substantial proportion of gut bacteria are considered 'unculturable'[25], there is a need to optimize culturing methods in order to expand our understanding of the *Clostridium* species.

Microbial cultivation remains indispensable for isolating specific bacterial strains and providing a continuous supply of cells for phenotypic and genetic analyses. This approach enables the determination of bacterial features, such as growth characteristics, physiology, and metabolism, as well as the interactions between these features[26]. With cultivation, the functional attributes of bacteria inferred from genomic data could be validated in experiments, improving reproducibility and statistical confidence[27]. Compared with aerobic bacteria, obligate anaerobic bacteria from the gut of GPs are more difficult to culture. Fecal samples must be collected and processed in an oxygen-free environment immediately after defecation to minimize exposure to air. Additionally, the diversity of cultivable strains is strongly influenced by media selection and formulation. Although previous researches have established optimized culture strategies for isolating gut anaerobes from humans, monkeys, and mice[28–30], including the development of appropriate selective media, physicochemical parameters, and growth factors, these approaches remain largely untested for giant pandas (GPs). The specialized bamboo diet of GPs creates a unique intestinal microenvironment with distinct nutritional requirements that differ from those of humans or model animals. This emphasizes the importance of developing culture media that better mimic the gut environment of GPs.

Although targeted isolation methods have successfully recovered specific *Clostridium* species from human and animal guts[31,32], including the isolation of *C. butyricum* from GPs[11], few studies have systematically evaluated the cultivable diversity and functional characteristics of *Clostridium* in GPs.

In this study, we optimized the anaerobic culture conditions for *Clostridium* to assess the diversity, composition and genomic feature of culturable *Clostridium* in GPs of different age groups (sub-adult, adult, and geriatric). The genotype and phenotype of the *Clostridium* strains, as well as their lignocellulose-degrading capabilities, were assessed. We further investigated the prevalence of VFs and ARGs to provide a better understanding of the functional and pathogenic potential of *Clostridium* species in the GP gut microbiome.

Results

Cultured *Clostridium* from the gut of GPs

Duplicate *Clostridium* species from the same samples isolated via the same cultural strategy (e.g., isolated from GAM without pre-incubation) were removed. In total, 98 *Clostridium* isolates were used to assess the various cultural strategies (Supplementary Table 1). Based on the alignment of 16S rRNA gene sequences against the EzBioCloud and NCBI BLAST databases (with a >97.0% similarity threshold for species assignment), the isolates were classified into 14 *Clostridium* species, including *C. perfringens* ($n = 25$), *C. sardiniense* ($n = 19$), *C. baratii* ($n = 11$), *C. nigeriense* ($n = 9$), *C. paraputrificum* ($n = 7$), *C. butyricum* ($n = 6$), *C. neonatale* ($n = 5$), *C. sporogenes* ($n = 5$), *C. saudiense* ($n = 3$), *C. ihumii* ($n = 2$), *C. moniliforme* ($n = 2$), *C. tertium* ($n = 2$), *C. carnis* ($n = 1$), and *C. sartagoforme* ($n = 1$). The most prevalent species detected among GPs were *C. perfringens* (61.29%, 19/31), *C. sardiniense* (45.16%, 14/31), and *C. baratii* (29.03%, 9/31).

We further compared the distribution of *Clostridium* species across different age groups (Fig. 1). In general, adult GPs ($n = 11$) exhibited a greater diversity of *Clostridium* species as compared to sub-adult ($n = 9$) and geriatric ($n = 6$) GPs. Three species, *C. perfringens*, *C. sardiniense*, and *C. sporogenes*, were common to all age groups. In contrast, *C. carnis* and *C. moniliforme* were only isolated from adult GPs, and *C. sartagoforme* and *C. saudiense* were only isolated from geriatric GPs.

Evaluation of the culture conditions for *Clostridium* isolation

Here, we found that 72 isolates, representing 14 species, were obtained with pre-incubation treatment, whereas 27 isolates, representing 7 species, were isolated without pre-incubation treatment (Fig. 2). Considering the effect of culture agars, most *Clostridium* species were produced from TM ($n = 10$), followed by RCM ($n = 9$) and GAM ($n = 8$). Fewer *Clostridium* species were isolated from CM ($n = 6$) and YCFA ($n = 3$). The results further illustrated that *C. sartagoforme* and *C. carnis* were exclusively recovered from GAM

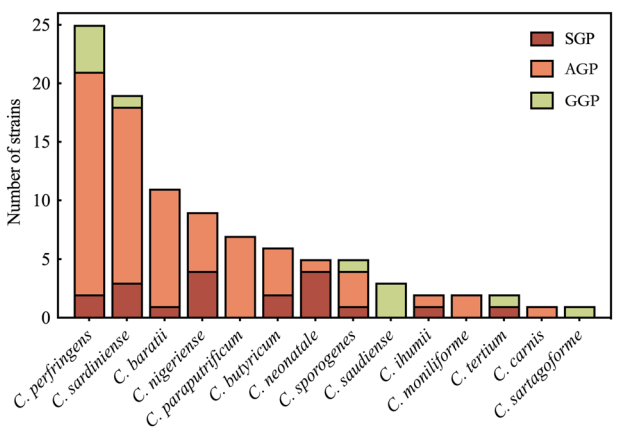

Fig. 1 | Distribution of *Clostridium* species in the gut of giant pandas at different ages. SGP: sub-adult giant panda, AGP: adult giant panda, GGP: geriatric giant panda.

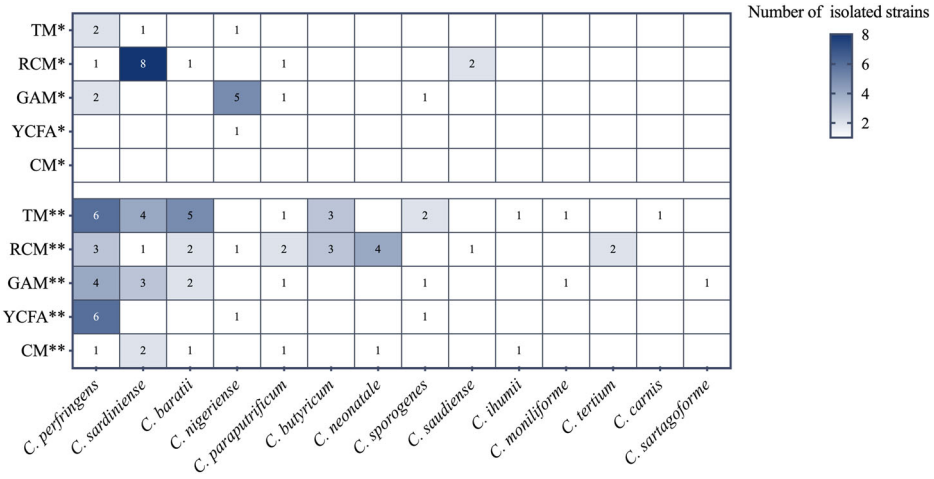

Fig. 2 | Effect of different culture strategies and media on the isolation of *Clostridium*. TM: thioglycollate medium, GAM: Gifu anaerobic medium, RCM: reinforced clostridial medium, YCFA: YCFA medium, CM: Columbia medium. *Without pre-incubation treatment; **with pre-incubation treatment.

and TM agars, respectively, and *C. saudiense* and *C. tertium* were isolated only from RCM agar.

Without pre-incubation treatment, RCM ($n = 5$) and GAM ($n = 3$) agar obtained the most *Clostridium* species, whereas fewer *Clostridium* species were identified from YCFA ($n = 1$) and TM ($n = 3$) as compared to RCM or GAM agar. However, no *Clostridium* was detected on CM agar. Under pre-incubation treatment, we found that more *Clostridium* species grew on RCM agar ($n = 9$) and TM agar ($n = 9$), followed by GAM agar ($n = 7$), CM agar ($n = 6$), and YCFA agar ($n = 3$). Additionally, all *Clostridium* species identified without pre-incubation treatment were also found after pre-incubation treatment, and 7 species, including *C. ihumii*, *C. butyricum*, *C. carnis*, *C. moniliforme*, *C. neonatale*, *C. sartagoforme*, and *C. tertium* were only identified after pre-incubation enrichment conditions. Of note, the combination of RCM, TM, and GAM with pre-incubation isolated all 14 *Clostridium* species. Thus, the combination of pre-incubation strategies and certain culture media was effective in increasing both the diversity and richness of culturable *Clostridium*.

Analysis of lignocellulose degradation

After dereplicating the initial collection of 98 Clostridium strains (i.e., removing same-species isolates from the same GP), 73 strains were retained for further testing (SGP, $n = 17$; AGP, $n = 46$; GGP, $n = 10$). Notably, all of the *Clostridium* strains were identified via the primary screening as having the potential ability to degrade cellulose (79.45%, $n = 58$), hemicellulose (54.79%, $n = 40$), and lignin (57.53%, $n = 42$), as evidenced by exhibiting corresponding β-glucosidase, xylanase, and MnP activities (Fig. 3a). In the SGP and AGP groups, there were more *Clostridium* strains with cellulose-degrading ability than those with hemicellulose- and lignin-degrading abilities. Also, *Clostridium* strains with lignin-degrading ability were less prevalent than those with hemicellulose- and cellulose-degrading abilities in the GGP group. Most *Clostridium* (35.62%, $n = 26$) possessed all three types of lignocellulose enzymatic capabilities, followed by 34.25% ($n = 25$) showing two types, and 16.44% ($n = 12$) showing one type of activity. Additionally, 13.70% ($n = 10$) of *Clostridium* lacked the capacity to degrade lignocellulose (Fig. 3b). In the SGP group, all strains exhibited at least two enzymatic activities, with some strains demonstrating all three enzymatic activities. In the AGP and GGP groups, 84.44% and 80.00% of *Clostridium* strains, respectively, possessed at least one enzymatic activity, with a higher proportion of strains exhibiting two enzymatic activities (Fig. 3b). The mean value of β-glucosidase activity in the AGP group was higher than that in the SGP and GGP groups, whereas the mean value of xylanase and Mnp activities was lower than that observed in the SGP and GGP groups. However, three enzymatic activities did not show significant differences among the various groups ($p > 0.05$) (Fig. 3c).

The enzymatic activities for lignocellulose degradation varied among *Clostridium* species (Fig. 3d). All species, except *C. sartagoforme*, exhibited β-glucosidase activity, with particularly high enzymatic activity observed in certain strains of *C. nigeriense* ($n = 30.37$ U/mL), *C. paraputrificum* ($n = 20.19$ U/mL), and *C. sardiniense* ($n = 20.62$ U/mL). A higher level of xylanase activity was observed in certain strains of *C. butyricum* ($n = 30.49$ U/mL), *C. perfringens* ($n = 28.62$ U/mL), and *C. baratii* ($n = 28.55$ U/mL), whereas no detectable xylanase activity was observed in *C. carnis* and *C. moniliforme*. MnP activity assessment identified *C. perfringens* strains as the most efficient producers, whereas *C. sartagoforme*, *C. sardiniens*, and *C. moniliforme* strains displayed no detectable MnP activity. Statistical analysis of species with ≥5 measurable replicates revealed significantly higher MnP activity in *C. perfringens* compared to *C. baratii* ($p < 0.05$). Nine different *Clostridium* species with three lignocellulose enzymatic activities were observed. Interestingly, all *C. butyricum* strains tested showed activity for all three lignocellulose-degrading enzymes, underscoring its exceptional lignocellulolytic potential. In contrast, *C. sartagoforme*, *C. sardiniens*, and *C. moniliforme* lacked detectable activity for one or more enzymes, indicating their limited lignocellulose degradation capability.

Whole genome sequencing of lignocellulose-degrading *Clostridium*

General genomic features of strains. Genome sequencing was performed on 26 *Clostridium* strains exhibiting all three lignocellulose-degrading enzyme activities. All genomic data have been deposited in BioProject database at NCBI under accession number PRJNA1258569. The assembly statistics and genome characteristics are presented in Supplementary Table 2. There were 169–2691 contigs (734 in average) yielded from *Clostridium* strains, with the total length ranging from 2,802,519 to 5,458,347 bp (3,884,414 bp in average). The N50 of the assembled genomes ranged from 100,005 to 2,363,697 bp (852,980 bp in average). The GC content ranged from 26.95% to 31.44% (29.05% in average), and the number of coding sequences (CDS) ranged from 2632–4562 (3396 in average) in the *Clostridium* strains.

Functional analyses of lignocellulose-degrading *Clostridium*

We annotated the genes of the *Clostridium* strains using the CAZy and KEGG databases to better understand their functions. There were 4294 genes identified to encode 211 CAZyme families, in which most were related to glycoside hydrolases (GHs) ($n = 114$), followed by carbohydrate-binding protein module (CBM) ($n = 41$), glycosyl transferases (GTs) ($n = 28$), polysaccharide lyases (PLs) ($n = 9$), carbohydrate esterases (CEs) ($n = 14$), and auxiliary activities (AAs) ($n = 5$). We further analyzed 41 CAZyme families that exhibited potential activity in degrading lignocellulose, including 30 GHs, 7 CEs, and 4 AAs (Fig. 4). Among these, we found that 28 of the 41 CAZyme families were involved in hemicellulose degradation, harboring enzymes, such as acetylxylan esterase (EC 3.1.1.72), xylan

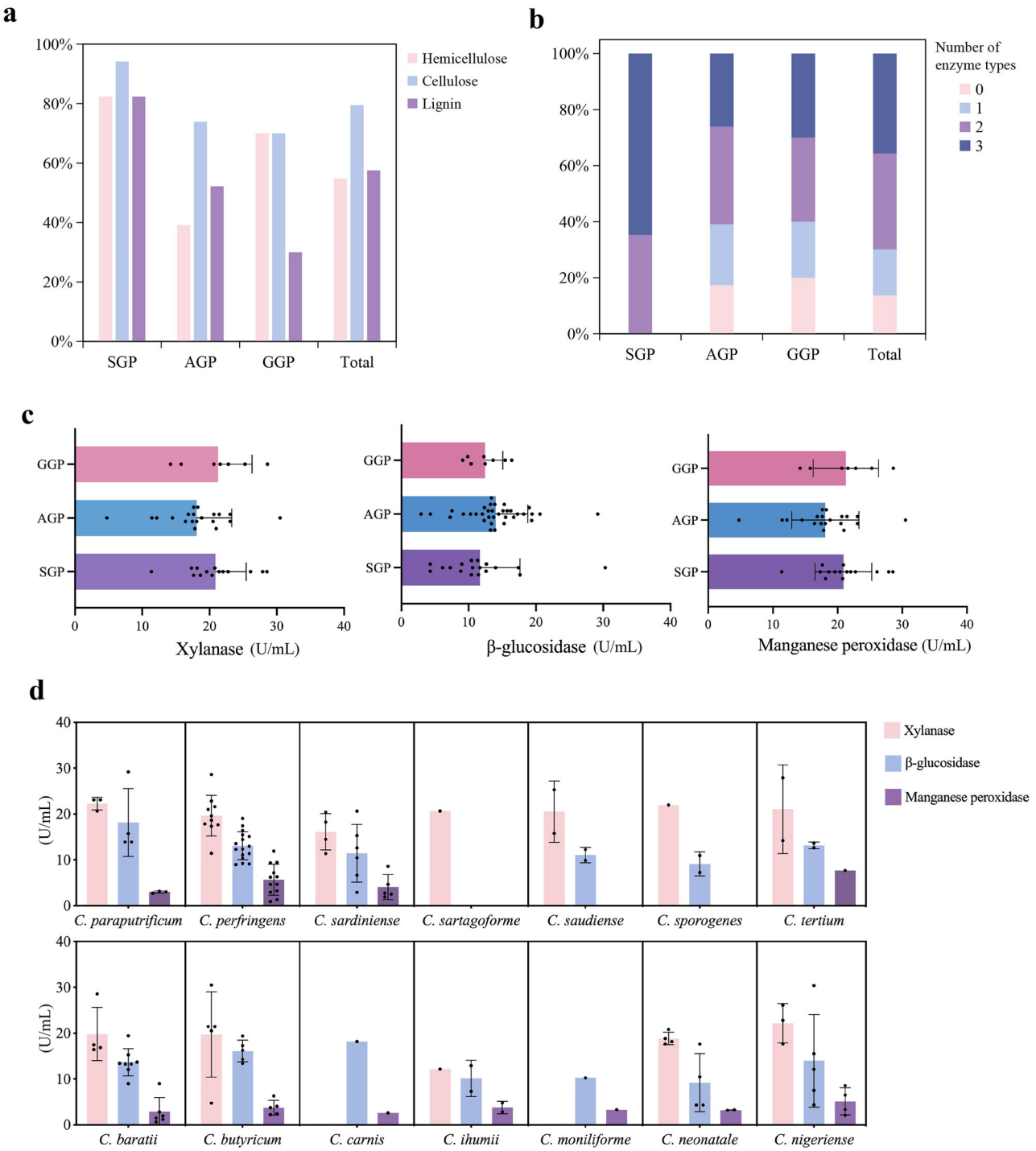

Fig. 3 | Analysis of lignocellulose degradation in *Clostridium*. **a** Prevalence of cellulose-, hemicellulose-, and lignin-degrading abilities in *Clostridium* isolated from giant pandas of different ages via primary screening. **b** Proportion of *Clostridium* strains by enzyme type (β-glucosidase, xylanase, and MnP activities) in different age groups. **c** Determination of xylanase, β-glucosidase, and manganese activities (U/mL) in the different age groups of giant pandas. Data are presented as mean ± SD. **d** Determination of xylanase, β-glucosidase, and manganese activities (U/mL) from different *Clostridium* species. Data are presented as mean ± SD. SGP: sub-adult giant panda, AGP: adult giant panda, GGP: geriatric giant panda.

β-1,4-xylosidase (EC 3.2.1.37), acetylesterase (EC 3.1.1.6), endo-β-1,4-xylanase (EC 3.2.1.8), α-L-arabinofuranosidase (EC 3.2.1.55), and feruloyl esterase (EC 3.1.1.73). The CE4 (acetylxylan esterase), CE1 (feruloyl esterase, acetylxylan esterase), and CE3 (acetylxylan esterase) families were present in all *Clostridium* strains. Enzymes, such as endo-β-1,4-glucanase (EC 3.2.1.4), β-glucosidase (EC 3.2.1.21), exo-β-1,4-glucanase (EC 3.2.1.74), exo-β-1,3-glucanase (EC 3.2.1.58), cellobiohydrolase (EC 3.2.1.91), and cellodextrinase (EC 3.2.1.74)—all related to cellulose breakdown—were found in 15 CAZyme families, with GH1 (exo-β-1,4-glucanase, cellodextrinase, β-glucosidase), and GH4 (β-glucosidase) exhibiting the highest gene counts. Additionally, we identified 6 CAZyme families involved in both cellulose and hemicellulose degradation. Furthermore, 4 AA families (AA1/2/4/6) with [copper-containing] dihydrogeodin oxidase (EC 1.10.3.-), laccase (EC 1.10.3.2), manganese peroxidase (EC 1.11.1.13), *p*-benzoquinone reductase (NADPH) (EC 1.6.5.6), and vanillyl-alcohol oxidase (EC 1.1.3.38), which all contribute to lignin degradation, were observed. The

Fig. 4 | Distribution of CAZymes associated with lignocellulose degradation in different species.

number of CAZyme families varied greatly among *Clostridium* strains, ranging from *C. ihumii* A467 ($n = 7$) to *C. neonatale* B160 ($n = 27$). Within the same species, several similarities were found. For instance, several CAZyme families, including GH43_4/43_10/10/115/30_2/67, which are all involved in the breakdown of hemicellulose, were specific to *C. neonatale*. Additionally, *C. butyricum* was shown to have more CAZyme families involved in cellulose breakdown, with GH5_44 and GH16_21 being unique to this species.

Of all *Clostridium* strains, a total of 245 KEGG pathways were obtained and assigned into 6 categories at KEGG level 1. The majority of these pathways were associated with metabolism ($n = 97–112$), followed by human diseases ($n = 35–41$), and organismal systems ($n = 21–29$). Fewer pathways were linked to genetic information processing ($n = 14$), environmental information processing ($n = 12–15$), and cellular processes ($n = 11–17$). This distribution underscores the central role *Clostridium* plays in metabolic functions within the gut of GPs. Subsequently, we focused on the top 35 enriched metabolic pathways, which were selected based on their highest average gene counts across all tested genomes. As shown in Fig. 5a, the number of functional genes in each metabolic pathway was consistent in strains within the same species. Notably, *C. butyricum* and *C. neonatale* harbored a greater abundance of functional genes, whereas *C. perfringens* and *C. baratii* displayed comparatively fewer. These pathways were classified into 7 categories at KEGG level 2, with the majority of genes enriched in carbohydrate metabolism. The key enzymes involved in the pathway of hemicellulose (xylan, mannose, and galactose) digestion were identified, including xylan 1,4-beta-xylosidase [EC 3.2.1.37], mannose PTS system EIIA component [EC:2.7.1.191], mannose-6-phosphate isomerase [EC:5.3.1.8], aldose 1-epimerase [EC:5.1.3.3], galactokinase [EC:2.7.1.6], UDPglucose--hexose-1-phosphate uridylyltransferase [EC:2.7.7.12], and phosphoglucomutase [EC:5.4.2.2] (Fig. 4b). Similarly, cellulose-digesting enzymes, such as endoglucanase [EC:3.2.1.4], beta-glucosidase [EC:3.2.1.21], cellobiose PTS system EIIA component [EC:2.7.1.205], 6-phospho-beta-glucosidase [EC:3.2.1.86], and glucokinase [EC:2.7.1.2], were detected (Fig. 5b). The distribution of these enzymes varied among different species, with *C. butyricum* exhibiting more diverse enzymes associated with hemicellulose and cellulose degradation (Fig. 4c). Furthermore, the metabolic products, glucose and fructose, could be fermented to produce short-chain fatty acids (SCFAs)—in particular acetate, propionate, and butyrate—as minor end-products. Within the "amino acid metabolism", enrichment was observed in arginine biosynthesis and lysine biosynthesis pathways. *Clostridium* species mainly facilitated arginine synthesis via KEGG module M00028 (glutamate => ornithine) and KEGG module M00844 (ornithine => arginine) (Fig. S1), whereas lysine synthesis was mediated via KEGG module M00016 (succinyl-DAP pathway, aspartate => lysine) and M00527 (DAP aminotransferase pathway, aspartate => lysine) (Fig. S1). Additionally, genes linked to the "metabolism of cofactors and vitamins" were also identified in pathways, such as porphyrin metabolism and folate biosynthesis.

Antibiotic resistance genes in *Clostridium*

In general, 197 genes belonging to 19 types of ARGs were annotated in the genomes of *Clostridium* strains isolated from the gut of GPs (Fig. 6). Most types of ARGs were related to glycopeptide resistance (*van*G/H/R/T/W/XY/Y), followed by tetracycline resistance [*tet*(Q), *tet*A(P), and *tet*B(P)], multidrug resistance (*cpl*R, *sdr*M, and *erm*Q), and disinfectant resistance (*qac*G and *qac*J). Additionally, the genes *gyr*B, *bla*R1, *aph* (3'), and *mpr*F, which may confer resistance to fluoroquinolone, beta-lactam, aminoglycoside, and peptides, were also observed. Antibiotic target alteration (52.63%, 10/19) was the major resistance mechanism of these ARGs, followed by antibiotic efflux (21.05%, 4/19), antibiotic target protection (15.79%, 3/19), and antibiotic inactivation (10.53%, 2/19). All strains, except *C. butyricum* A511, possessed the genes *van*W and *van*T; the genes *van*Y (73.08% 19/26), *cpl*R (61.54%, 16/26), and *gyr*B (53.85%, 14/26) were also prevalent. The distribution and prevalence of ARGs varied by *Clostridium* species. For example, more types of ARGs ($n = 7–9$) were enriched in *C. perfringens*, whereas *C. butyricum* A511 had only 2 ARGs, *tet*A(P) and *tet*B(P). The genes *van*H and *mpr*F were unique in *C. perfringens* strains, and *van*G, *van*R, and *aph*(3') were only detected in *C. ihumii* A467.

Furthermore, based on the KEGG analysis of pathways related to antibiotic resistance, we found that most genes were involved in β-lactam resistance (ko01501), and vancomycin resistance (ko01502) was the most abundant among all strains. *Clostridium* strains that resist β-lactam could result from the regulation of the *bla*Z gene, which encodes a class A β-lactamase enzyme to hydrolyze the β-lactam ring, or the alteration of the β-lactam targets of penicillin-binding proteins (PBPs), including *PBP*1a/2, *PBP*2, and *fts*I. Vancomycin resistance pathway is regulated by *van*R and *van*S (*Van*S-*Van*R two-component system), and several KOs, such as K01929 (*murF*), K01000 (*mraY*), K02563 (*murG*), K01921 (*ddl*), and K01775 (*alr*), are involved to prevent vancomycin binding by replacing the D-alanyl-D-alanine (D-Ala-D-Ala) target to either D-alanyl-D-lactate (D-Ala-D-Lac) or D-alanyl-D-serine (D-Ala-D-Ser), which results in different levels of resistance to vancomycin.

Prevalence of virulence factors in *Clostridium* strains isolated from GPs

All strains comprised 23 VFs expressed by 408 VGs, which could be categorized as follows: adherence ($n = 7$), exoenzyme ($n = 4$), immune modulation ($n = 4$), exotoxin ($n = 4$), motility ($n = 2$), regulation ($n = 1$), and stress survival ($n = 1$) (Fig. 7). Of these, the adherence VFs were more prevalent among *Clostridium* strains, whereas the VFs, EF-Tu and GroEL, were shared by all strains. The Streptococcal plasmin receptor/GAPDH and FbpA/Fbp68 were found in 92.31% (24/26) and 53.85% (14/26) of strains, respectively. The majority of VFs related to exoenzyme, exotoxin, and regulation were predominantly identified in *C. perfringens*. Of particular interest were the VFs that were uniquely found in all strains of *C. perfringens*, including alpha-clostripain, kappa-toxin, mu-toxin, alpha-toxin (CpPLC), and the VirR/VirS two-component system. Additionally, most VGs were found in type IV pili ($n = 83$), mu-toxin ($n = 62$), and EF-Tu ($n = 46$), in which type IV pili covered most types ($n = 16$), including *pil*A/M/N/T. Additionally, the most frequently detected VGs in strains were *tuf*A (EF-Tu, 46/408) and *gro*EL (GroEL, 26/408).

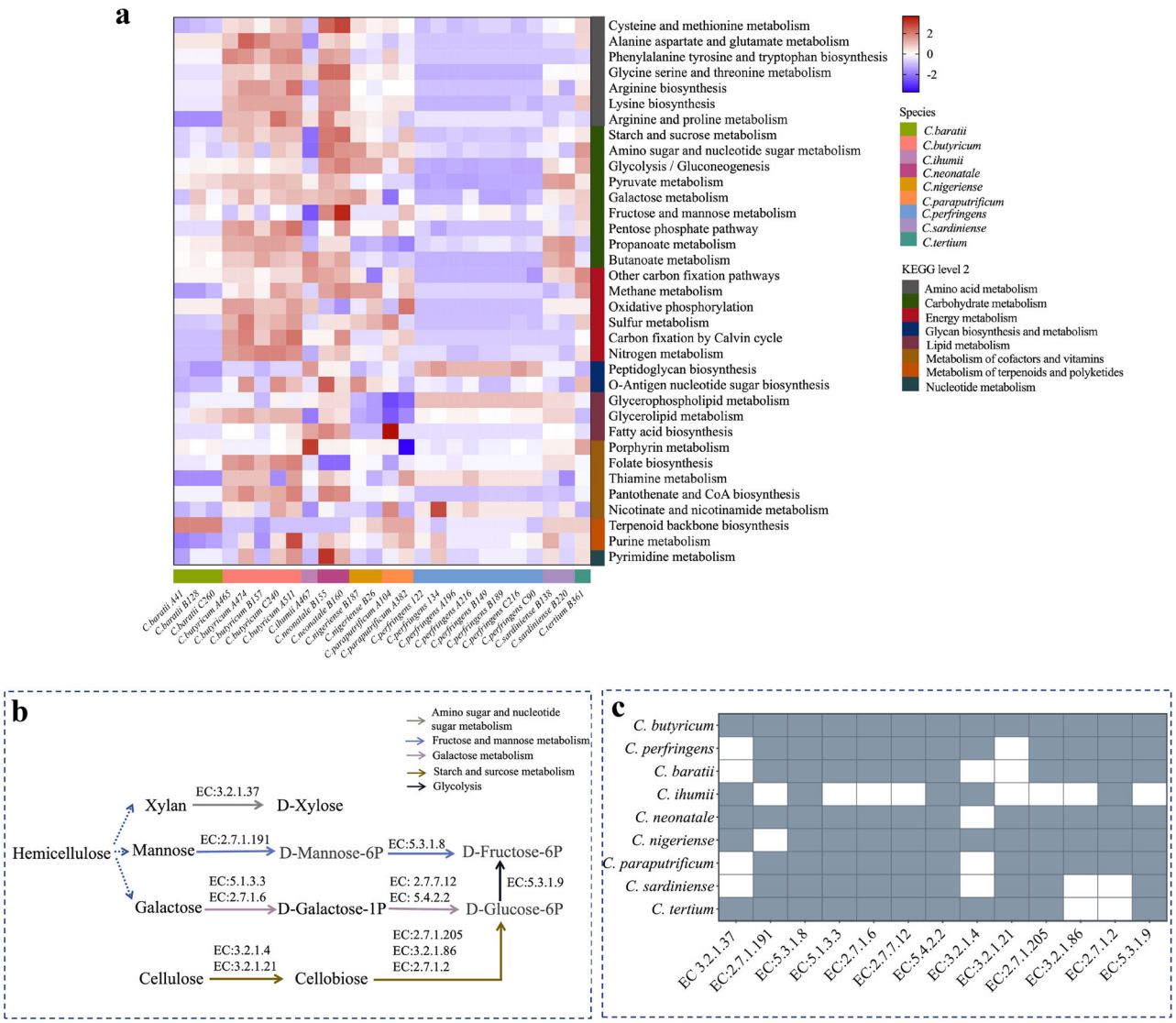

Fig. 5 | KEGG analysis of lignocellulose degradation by *Clostridium* in the gut of giant pandas. a Distribution of metabolic pathways enriched in various *Clostridium* species. The gene counts were normalized using *z*-scores (scale from −2 to +2). **b** Key enzymes in the metabolic networks involved in hemicellulose and cellulose degradation. **c** Distribution of key enzymes involved in hemicellulose and cellulose degradation in various *Clostridium* species. White grids represent species without the enzyme; gray-blue grids represent species with the enzyme.

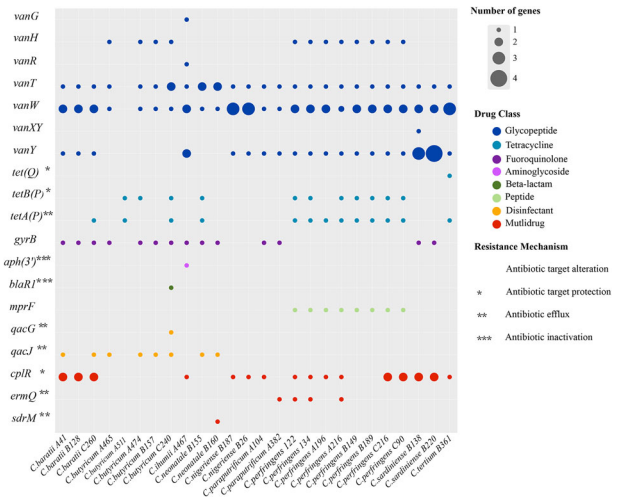

Fig. 6 | Distribution of antibiotic resistance genes found in *Clostridium* strains.

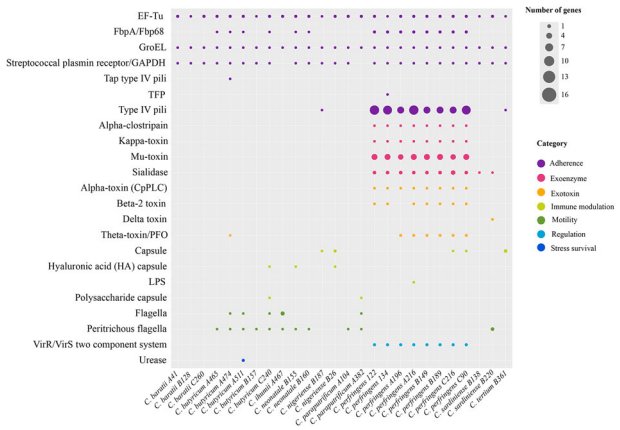

Fig. 7 | Distribution of virulence factors found in *Clostridium* strains.

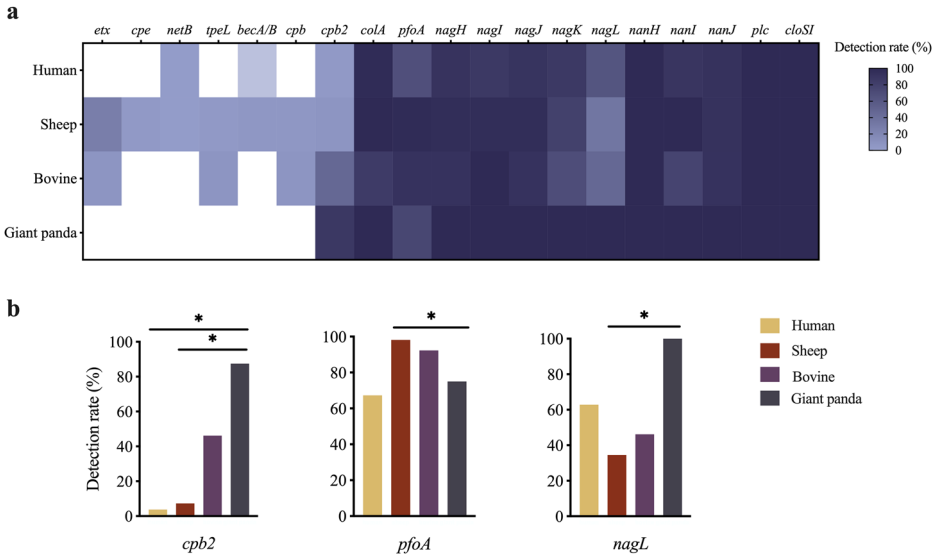

Fig. 8 | Comparison of toxin genes in *Clostridium perfringens* from giant pandas with humans and herbivores. a Detection rate of toxin genes from different hosts. **b** Significantly different detection rates of toxin genes between giant pandas and humans and herbivores were observed.

Given that the VGs of toxins, which are largely distributed in *C. perfringens*, are responsible for disease pathogenesis, we further compared the prevalence of toxin genes in *C. perfringens* strains from herbivores (sheep and bovine) and humans as previously studied (Supplementary Table 3)[32]. Our results indicated that the majority of toxin genes were found in *C. perfringens* strains isolated from sheep, followed by bovine, human, and GPs. All 13 toxin genes observed in GPs were also found either in herbivores or humans (Fig. 8a). The detection rates varied among different toxin genes. All strains from GPs, herbivores, and humans had *nan*H, *plc*, and *clo*SI, whereas only 3.64% of *C. perfringens* strains from sheep had the *cpe* gene. The detection rate of *cpb*2 in *C. perfringens* strains from GPs was significantly higher compared to sheep and humans, and the detection rate of *nag*L in *C. perfringens* strains from GPs was significantly higher than in sheep. The detection rate of *pfo*A in *C. perfringens* strains from GPs was significantly lower than in sheep (Fig. 8b).

Potential mobile genetic elements in genomes

A total of 260 transposases were annotated among genomes (Supplementary Table 4), in which 99 transposases were classified in 16 different *IS* families, with the majority being found in *IS*3 ($n = 19$), *IS*200/*IS*605 (n = 18), and *IS*1595 ($n = 15$) transposase families. The maximum number of transposases was found in two *C. neonatale* strains (B155, $n = 26$; B160, $n = 24$), whereas the lowest number was found in the two *C. baratii* strains (n = 2). The number of transposases in different strains of *C. perfringens* ($n = 3$–20) and *C. butyricum* ($n = 5$–22) varied significantly. Some *IS* families were found to be shared among genomes. For example, *IS*3 and *IS*200/*IS*605 were prevalent in 42.31% (11/26) and 38.46% (10/26) of strains, respectively. Additionally, *IS*L3, *IS*91, *IS*701, and *IS*1470 transposase families were uniquely identified in different strains. Furthermore, we examined the genetic background of transposase in contigs of strains to investigate the potential risk of ARGs and VGs dissemination (Fig. 9). We found that the peptide gene, *mpr*F, had a similar genetic background in three *C. perfringens* (122, 134, C90) and was distributed upstream of transposase *ins*Q, and *C. perfringens* A216 had the *van*Y genes downstream of *ins*Q. The distribution of *van*Y in four *C. perfringens* strains (122, 134, C90, and C216) was similar, as it sequentially associated with the IS200/IS605 family element transposase accessory protein *tnpB*.

Discussion

Clostridium is a heterogeneous genus of obligate anaerobes belonging to the phylum Firmicutes, which comprises over 300 species (data collected in EzBioCloud database, https://www.ezbiocloud.net/). Different *Clostridium* patterns have been cultivated from a variety of habitats, such as human and

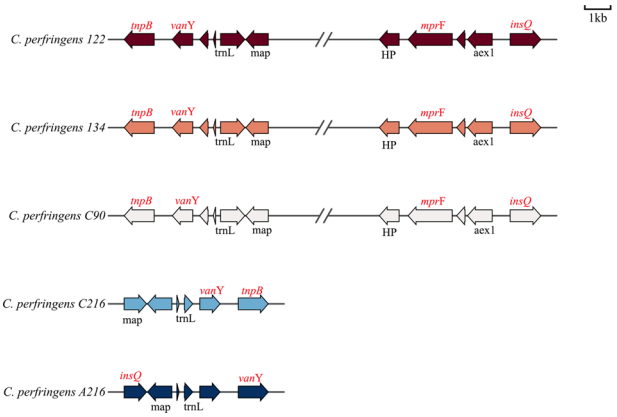

Fig. 9 | The genetic environment of antibiotic resistance and virulence genes associated with transposase.

animal intestine, soil, and mud pits[28,29,33,34]. To improve our understanding of difficult-to-culture *Clostridium* species and their functions in the guts of GPs while optimizing experimental efficiency, we systematically evaluated culture conditions through parallel comparison of pre-incubation versus non-pre-incubation approaches, and comparative assessment of isolation media types. Our findings demonstrate the effect of a pre-incubation strategy on enhancing bacterial diversity, which aligns with a previous study that highlighted the benefit of culture enrichment in increasing bacterial species[35]. While Lagier et al. recommended that fecal extraction and sheep blood are crucial growth enhancers in blood culture bottles for human gut anaerobes[36], we found pre-incubation in GAM liquid media or blood culture bottles containing sheep blood failed to enhance species diversity compared to RCM and TM liquid media without sheep blood. This underscores the variability in optimal cultivation conditions across different samples, which requires considerable work to screen for appropriate conditions[37]. Through comparative analysis of five media types commonly used in anaerobic culturing[24,31], we identified suboptimal media that could be excluded from further isolation workflows. Ultimately, this study indicated that a combination of pre-incubation and RCM, TM, and GAM agar yielded the highest number of species, providing a valuable reference for standardizing *Clostridium* isolation protocols in GP gut microbiota research.

Compared with culture-independent studies regarding the *Clostridium* composition in the gut of GPs[4,6], the culture-dependent approach used in this study allowed for outcomes of more *Clostridium* species, such as *C.*

sardiniense, *C. carnis*, *C. ihumii*, and *C. moniliforme*, thereby expanding the catalog of gut *Clostridium* genomes in GPs. Under normal circumstances, *Clostridium* species in the gastrointestinal tract play complex physiological functions and establish a symbiotic relationship with the host[14]. Based on this, a wide range of mechanistic studies have been conducted in order to improve the development of microbial therapies that maintain gut homeostasis[10]. As one of the most promising probiotics, evidence on the roles that *C. butyricum* plays in treating intestinal conditions, such as intestinal injury, irritable bowel syndrome, inflammatory bowel disease, and colorectal cancer, has been summarized[38]. *C. butyricum* mediates tolerogenic APC signaling to increase the Treg response, which in turn suppresses proinflammatory effector T cell responses when pathogenic or inflammatory circumstances are present in the intestinal epithelium[38]. Previous studies have suggested that the *C. butyricum* isolated from GP feces alleviates colitis in mice by increasing the expression of intestinal barrier proteins and the abundance of probiotic species and by inhibiting immune responses[11]. Furthermore, the main metabolite of the intestinal epithelium, butyrate, not only reduces epithelial damage in the colonic tissue of diarrhea mice by increasing mucin production via enhancing the expression of the *MUC* gene[39], but also potentially by increasing the body weight of GPs by upregulating the hepatic circadian gene to promote lipid biosynthesis[40]. In this study, we isolated *C. butyricum* from the gut of SGPs and AGPs, but not from GGPs. This might suggest a lower prevalence of *C. butyricum* with age. With advancing age, GPs experience gastrointestinal function decline and tooth wear, which impair crude fiber (CF) digestion through reduced chewing efficiency and intestinal processing. Given the well-documented probiotic properties of *C. butyricum*—particularly its immunomodulatory effects, butyrate production, and demonstrated lignocellulolytic activity—dietary supplementation in GGPs may ameliorate age-related gut dysfunction while enhancing bamboo digestion and nutrient utilization capacity. We therefore propose that *C. butyricum* supplementation represents a promising nutritional strategy to maintain both intestinal homeostasis and digestive efficiency in GGPs. Additionally, *C. sporogenes*, which was observed across all age groups, has demonstrated probiotic potential as its bioactive metabolite indole-3-propionic acid (IPA) helps skeletal muscle development and protects against chronic inflammation[41]. Taken together, it is valuable to further investigate the mechanisms of *Clostridium* on molecular responses and nutrient utilization in order to better understand how *Clostridium* species benefit GPs.

Although all *Clostridium* strains we obtained are a normal component of the gut microbiome from healthy GPs, several species isolated, including *C. perfringens*, *C. paraputrificum*, and *C. tertium*, have been reported as potentially hazardous agents to humans and/or animals in certain cases[42–44]. As one of the most important opportunistic pathogens, *C. perfringens* can cause several gastrointestinal diseases, such as necrotic enteritis, enterotoxemia, and enterocolitis, primarily due to its ability to produce various toxins[45,46]. The short generation time of *C. perfringens*, doubling within 10 min under optimal conditions[47], likely contributes to its high isolation rate in GPs and may exacerbate disease progression. These findings highlight the dual nature of *Clostridium* species in the gut of GPs, encompassing both beneficial effects and potential health risks. Further research is warranted to elucidate the balance between these opposing roles and their implications for GP health management.

Symbiosis with a lignocellulose-degrading microbiome appears to compensate for an inability to generate lignocellulolytic enzymes in GPs[5]. Compared with fungi, bacteria exhibit several advantages in lignocellulose degradation, including higher growth rate, broad substrate specificity, and easy expression of multi-enzyme complexes[48]. These attributes position bacteria as promising candidates for the efficient degradation and utilization of lignocellulosic biomass in various biotechnological applications. Under anaerobic conditions, *Clostridium* proliferates on the surface of organic matter, releasing complex enzymes to degrade lignocellulose and further transform it into SCFAs, such as acetate, butyrate, and propionate, that the host needs[49]. Previous high-throughput sequencing studies have revealed *Clostridium* as a main resource for cellulose degradation among gut bacteria in GPs[12,50]. Likewise, our results regarding in vitro lignocellulose enzyme assays in combination with genome analysis of lignocellulose-degrading enzymes strongly suggested that the *Clostridium* in the gut of GPs secrete multiple enzymes to support lignocellulose metabolism. The types of CAZyme families associated with hemicellulose degradation were more than cellulose and lignin degradation, which may be because the complexity of the composition of hemicellulose requires the action of a wide set of enzymes[51]. Key enzymes involved in cellulose degradation, such as β-glucosidase (EC 3.2.1.21), endo-β-1,4-glucanase (EC 3.2.1.4), and cellobiohydrolase (EC 3.2.1.91), are distributed in various GH families (e.g., GH1, GH4, GH8, GH39, GH30_1, GH51_1, GH16_21). These enzymes act synergistically at various stages of cellulose hydrolysis, ultimately converting cellulose into glucose, which is readily absorbed by the host[52]. Lignin is a heterogeneous aromatic heteropolymer that binds cellulose and hemicellulose and is quite recalcitrant to degradation[53]. Our primary screening revealed a reduced incidence of lignin-degrading *Clostridium* in GGPs as compared to SGPs and AGPs. A prior study discovered that GGPs who consumed more bamboo shoots and less bamboo had a lower intake and digestion of crude fiber[54]. Hence, we theorized that the reduced lignin-degrading ability of *Clostridium* in GGPs could be due to their lower bamboo fiber intake. In return, a higher prevalence of lignin-degrading *Clostridium* in SGPs and AGPs may reflect an adaptive evolution to a higher fiber diet. As one of the best characterized lignin-modifying enzymes, the activity of MnP was detected in all strains with potential lignin-degrading ability, which has the capacity of converting lignin phenolic compounds to phenoxy radicals. In addition to lignin degradation, the ability of MnP to detoxify multiple mycotoxins, including aflatoxin, deoxynivalenol, and patulin[55], may aid GPs in the reduction of potential mycotoxins in food. However, MnP was represented with low prevalence in strains via CAZyme annotation, which could be due to the low copy number of these enzymes in the *Clostridium* genomes and/or the low number of representative sequences available in the CAZymes database[56].

The ability of *Clostridium* species to ferment a wide range of nutrients as chemoorganotrophic bacteria is widely recognized, and the majority of the metabolites they generate have multiple beneficial impacts on gut health[57]. In this study, we found a wide range of gut *Clostridium* in GPs with lignocellulose-degrading ability not only harbored a variety of genes related to SCFAs, but also contributed to the synthesis of essential amino acids via arginine and lysine biosynthesis pathways, thus serving as an energy source for a series of bodily functions. Arginine plays a central metabolic role as the biosynthetic precursor for several physiologically critical molecules, including nitric oxide, urea, ornithine, and citrulline. Nitric oxide particularly serves as a key regulator of both immune function and metabolic homeostasis, modulating glucose, fatty acid, and amino acid metabolism in mammalian systems[58,59]. Furthermore, lysine undergoes catabolism in mammalian systems to provide energy, while also serving as an essential precursor for numerous bioactive compounds, such as carnitine, glutamate, and collagen. Through these derivatives, lysine plays an indispensable role in cellular metabolism, energy homeostasis, and neural function[60]. These functional attributes of *Clostridium* may represent an evolutionary response to the bamboo diet of GPs, underscoring the role of the gut microbiota in strengthening the energy supply and maintaining metabolic homeostasis in GPs.

Since antibiotics are the most widely used and effective treatment for gastrointestinal disorders in GPs, it is inevitable that they may have side effects and exacerbate antibiotic resistance. Previous studies using metagenomic sequencing have gained insight into the overall distribution of ARGs within the gut microbiome of GPs, demonstrating that the ARGs mediated by the mechanism of antibiotic efflux were the most expressed[19,61]. The type of bacteria associated with the abundance and diversity of ARGs was also investigated previously[3]. For example, *E. coli* was recognized as the primary reservoir of ARGs, whereas specific *Clostridium* species were the main source of ARGs in wild GPs[6,19]. Additionally, using an aerobic culture-dependent approach, the antibiotic phenotype and genotype were monitored from the prevalent bacteria in GPs, such as *E. coli*, *Enterococcus* spp.,

Enterobacter spp., and *Klebsiella pneumoniae*, providing more precise guidance for appropriately prescribing antibiotics for diseases caused by specific bacterial infections[62]. Herein, we broaden the understanding of ARG distribution in *Clostridium*, a representative anaerobe in the gut microbiome of GPs. Our results demonstrated that *Clostridium* strains exhibit ARGs resistant to different classes of antibiotics, with the *van* genes, which act as a primary source of glycopeptide resistance determinants in environmental bacteria and pathogens[63], were most prevalent. Similarly, Mustafa et al.[64] also found a positive correlation between *Clostridium* and various *van* genes through the metagenome sequencing of gut bacteria in GPs. Glycopeptide antibiotics are a last resort in treating multidrug-resistant, gram-positive bacterial infections. These antibiotics work via binding to the D-Ala-D-Ala terminus of peptidoglycan, thus preventing the synthesis of the bacterial cell wall[65]. However, as the first therapeutically approved glycopeptide, long-term use of vancomycin triggered widespread bacterial resistance by the mechanism of antibiotic target alteration[66]. Notably, vancomycin is seldom used in clinical treatments for captive GPs, suggesting that the prevalence of genes in *Clostridium* is unlikely to be driven by direct antibiotic selection pressure. This conclusion is further supported by the previous identification of *Clostridium* as the primary reservoir of *van* genes in the gut microbiome of wild GPs[67], where antibiotic exposure is minimal. To further investigate the potential for horizontal transfer of these ARGs, we performed an analysis of mobile genetic elements (MGEs). Although the use of draft genomes assembled from short-read sequencing data can introduce a bias whereby MGEs are placed at contig termini, manual curation confirmed that all major MGEs associated with ARGs were located internally within large contigs. This important finding guarantees the integrity of their sequences and flanking genetic contexts. That said, it cannot be ruled out that ARGs on MGEs might be missed due to the presence of only draft genomes. Future studies with complete genome sequences will provide a more complete picture of ARGs on MGEs in the giant panda gut microbiome. Our genomic analysis indeed revealed that these *van* genes are physically linked to MGEs, indicating a high potential for horizontal gene transfer within species. Beyond this, recent studies suggest that resistance may also stem from complex environmental and dietary interactions[68]. Specifically, dietary bamboo has been identified as a reservoir of ARGs that harbors *van* genes, with MGE-mediated mechanisms facilitating their incorporation into the GPs' gut resistome[69]. Meanwhile, the shared presence of *van* genes and mobile genetic elements (MGEs) across bacterial communities in GP feces, dietary bamboo, and surrounding soil suggests their involvement in cross-species gene transfer[70]. Furthermore, metals are known to exert selection pressure promoting ARG proliferation in bacterial communities[71]. In GPs, identical metals detected in bamboo were consistently identified in gastrointestinal and fecal samples, along with significant associations observed among gastrointestinal metals, microbiome, metal resistance genes (MRGs), ARGs and MGEs[61]. Additionally, other studies have shown drug-resistant *Bacillus* carries a variety of copper resistance genes, *van* genes and MEGs in the plasmid that enables both vertical and horizontal gene transfer[72]. In summary, the available findings suggest *van* gene prevalence likely results from synergistic effects of dietary exposure to both resistance genes and metal selective pressures, combined with horizontal transfer from environmental and commensal bacterial reservoirs.

Bacteria use a variety of VFs to increase their ability to evade host defenses and transmit disease[73]. Our research demonstrated that most genes encoded VFs for adhesion, which may be the primary factor threatening the health of GPs. As the most prevalent VF, EF-Tu attaches to the host extracellular matrix components, such as plasminogen, fibronectin, mucins, and factor H, which can serve as effective adhesion targets for pathogens. EF-Tu facilitates invasion and colonization, aids immune system evasion, and increases virulence[74,75]. GroEL, a member of the heat-shock protein (HSP) family, is widely found in both prokaryotes and eukaryotes and primarily serves to increase bacterial heat tolerance. GroEL is also thought to be a critical molecule in infectious and inflammatory diseases induced by pathogens[76], and it acts as an adhesin for several pathogens, including *C. difficile* and *Chlamydia pneumoniae*, to aggravate specific diseases[77,78]. Moreover, *Cronobacter sakazakii* GroEL is characterized as an inflammation stimulator in the gut, which causes host cell necrosis by activating the NF-κB-signaling pathway to release more proinflammatory cytokines (TNF-α, IL-6, and IL-8), and assisting pathogens in crossing the intestinal barrier[79].

Notably, our findings revealed that *C. perfringens* is the main carrier of VFs. A number of type IV pili it encodes mediate adhesion to host cells[80], which help other VFs disrupt epithelial barrier function and induce histotoxic infections or tissue necrosis[17,81]. The different extracellular toxins and enzymes that *C. perfringens* produces are largely responsible for its pathogenicity. Previous studies have identified seven different types of *C. perfringens* toxins (A–G) based on the combination of six major toxins (α-toxin, β-toxin, ι-toxin, ε-toxin, *C. perfringens* enterotoxin, and necrotic enteritis B-like toxin)[32,45,82]. We found that all eight of the *C. perfringens* isolates listed here displayed comparable toxin production patterns, and they are all categorized as type A, which solely generates α-toxin. The α-toxin is a zinc-containing phospholipase C enzyme with the ability to hydrolyze cell membranes and impair the innate immune response[15,83]. The other non-typing toxins or extracellular degradative enzymes (e.g., beta-2 toxin, theta toxin, Mu toxin, and sialidase) enriched in *C. perfringens* are supposed to play an important role in colonization and immunomodulation, cell injury, and, as a result, are now coming under intensive validation study[83,84].

Though the commensal gut bacteria *Clostridium* in GPs exhibited carried VGs, it should be noted that the determinant of pathogenesis is not only dependent on the virulence factors encoded by the pathogen, but is also dependent upon several environmental stressors and accessory genes[85]. This could explain the presence of opportunistic pathogens, such as *C. perfringens*, in the guts of GPs or other healthy humans and animals[47,86]. Our findings offer some insight into the prevalence and horizontal transfer of ARGs and VGs in lignocellulose-degrading *Clostridium*, which could be useful in anticipating and averting the development of virulence and antibiotic resistance. The acquisition of ARGs and VGs may facilitate bacterial evolution and environmental adaptation, potentially enhancing the ecological fitness of these microorganisms. Furthermore, the presence of ARGs and VGs in *Clostridium* species may promote successful gut colonization and increase resistance to environmental stressors, thereby supporting their functional role in lignocellulose degradation within the gastrointestinal ecosystem. These findings contribute to our understanding of the complex interplay between genetic determinants and functional adaptation in the gut microbiota, particularly in relation to lignocellulose degradation processes.

Methods

Collection and processing of fecal samples

Fecal samples were collected from 31 GPs living in the China Conservation and Research Center for the Giant Panda (CCRCGP), including 7 sub-adult GPs (SGPs) (2–3 years old), 17 adult GPs (AGPs) (6–18 years old), and 7 geriatric GPs (GGPs) (21–29 years old) (Supplementary Table 5). All healthy individuals were fed a diet with a consistent composition and did not receive any drugs for at least 30 days prior to sampling. To preserve anaerobic conditions, freshly voided fecal samples were immediately transferred to sterile anaerobic gas-generating bags (Hope Bio-Technology Co., Ltd) and maintained at 4 °C during transport. All samples were processed within 2 h of collection in an anaerobic chamber (BactronEZ-2, SHELLAB, USA) under an atmosphere of 90% N_2, 5% H_2, and 5% CO_2 to maintain anaerobic conditions.

Culture strategy for *Clostridium*

Four different liquid media conditions and five different solid media conditions were used in this study, selected based on their established efficacy for gut anaerobe cultivation[24,31,87], manufacturer recommendations, and successful *Clostridium* isolation in our preliminary tests. Detailed information regarding the culture media and additives is presented in Supplementary Table 6. Fecal suspensions were prepared by homogenizing 10 g of the most unexposed inner part of each fecal sample in 50 ml of

phosphate-buffered saline (PBS) supplemented with 0.05% cysteine. Then, 5 ml of each fecal suspension was inoculated into 45 ml of various liquid culture enrichment media, including Gifu anaerobic medium (GAM), thiolglycollate medium (TM), reinforced clostridial medium (RCM), and anaerobic blood culture medium. Each culture was incubated at 37 °C in an anaerobic chamber. After 0 days (without pre-incubation) and 5 days (with pre-incubation) of anaerobic culture, 1 ml of liquid from the GAM, TM, or anaerobic blood culture was diluted, plated onto solid GAM, TM and YCFA plates, respectively, and then incubated at 37 °C under anaerobic conditions for 48–72 h. Also, 1 ml of liquid from the RCM culture was diluted and plated onto RCM and Columbia medium (CM) at 37 °C under anaerobic conditions for 48–72 h. Colonies with different appearances (e.g., color, size, and shape) were picked from each plate and purified in GAM agar at 37 °C under anaerobic conditions for 48 h. All purified isolates were amplified using universal 16S rRNA primers 27F (5′-AGAGTTTGATCMTGGCTCAG-3′) and 1492R (5′-TACGGYTACCTTGTTACGACTT-3′) and sequenced by Sangon Bioengineering Co., Ltd (Shanghai, China). Each strain was amplified using PCR three separate times. Then, PCR products were sequenced and aligned, confirming identical species identification with high reproducibility. Nucleotide sequences were analyzed using EzBioCloud (https://www.ezbiocloud.net) and NCBI. If multiple strains isolated from the same sample under the same culture conditions were identified as the same species, then one was randomly selected for further evaluation. Confirmed strains were stored in GAM broth containing 30% glycerol at −80 °C.

Primary screening of lignocellulose-degrading *Clostridium*

A dye decolorization assay was used to assess the isolated *Clostridium* for hemicellulose-, cellulose-, and lignin-degrading activity as previously described[88,89]. Three types of selective media containing xylan, carboxymethyl cellulose (CMC), or sodium lignin sulfonate as the sole carbon source were used to select isolates with potential hemicellulose-, cellulose-, and lignin-degrading activity, respectively. Detailed information on the media used is listed in Supplementary Table 6. Briefly, duplicate *Clostridium* species from the same GP were removed from analysis. The purified strains were evenly spread across GAM and incubated at 37 °C under anaerobic conditions for 48 h. Next, cylindrical agar blocks (5 mm in diameter) were excised from agar with confluent growth and placed on selective media. The agar plate containing the agar block was incubated at 37 °C under anaerobic conditions for 48 h. The *Clostridium* species with hemicellulose-, cellulose-, and/or lignin-degrading ability were indicated by decolorization zones. The isolates that exhibited decolorization zones in triplicate were selected to be assayed by a lignocellulose enzyme assay.

Lignocellulose enzyme assay

To quantitatively verify the bamboo lignocellulose degradation activity, the *Clostridium* species with potential hemicellulose-, cellulose-, and/or lignin-degrading activity were identified by testing their β-glucosidase, xylanase, and manganese peroxidase (MnP) activity, respectively. Briefly, bamboo stem and leaf (*Pleioblastus amarus*) were dried at 40 °C and then ground and passed through a 50-mesh sieve. To minimize the effect of the bamboo microbiome on the enzyme assay, bamboo powder was irradiated using a Coalt-60 gamma irradiator with doses of 8.00 kGy (Zhongjin Irradiation Co., Ltd.). No surviving colonies were detected in the bamboo powder after radiation. Subsequently, single colonies of each strain were inoculated into GAM broth and incubated at 37 °C under anaerobic conditions for 24 h. Then 1 ml of the bacterial suspension (OD_{600} = 0.6) was added to bamboo fermentation broth (Supplementary Table 6) containing 5% (w/v) bamboo powder as the sole carbon source. After 24 h of anaerobic incubation, the bamboo fermentation solution was centrifuged (8000 × *g*, 10 min, 4 °C) and the supernatant was collected for enzymatic analyses. Enzyme activity was quantified using commercial assay kits (Solarbio, China) following the manufacturer's protocols, with absorbance measurements performed on a Varioskan LUX multimode microplate reader (Thermo Scientific, USA); β-glucosidase activity (BC 2560) was measured via the *p*-nitrophenyl-β-D-glucopyranoside hydrolysis method, with the enzymatic release of *p*-nitrophenol quantified at 400 nm; neutral xylanase activity (BC 2595) was assessed using the 3,5-dinitrosalicylic acid (DNS) method based on reducing sugar release from xylan substrate and quantified at 540 nm; and MnP activity (BC 1625) was determined by monitoring the enzymatic oxidation of guaiacol to tetraguaiacol at 465 nm in the presence of Mn^{2+}. Each strain was analyzed using enzyme activity assays three separate times, with the final enzymatic activity value representing the mean of the three measurements.

Whole-genome sequencing of lignocellulose-degrading *Clostridium*

The genomic characteristics of those *Clostridium* strains that possessed all three tested enzymatic activities were subjected to further analysis. Total genomic DNA of *Clostridium* was extracted using the DNeasy Blood and Tissue Kit (Qiagen) according to the manufacturer's instructions. The sequencing library was generated using NEB Next® UltraTM DNA Library Prep Kit for Illumina (NEB, USA), and the library quality was verified by Qubit®3.0 Flurometer (Invitrogen, USA) and NGS3K/Caliper. After sequencing on an Illumina PE150 platform (150-bp paired-end reads) in Novogene, the raw reads were trimmed to remove low-quality reads via Trimmomatic, and the de novo assembly was performed using SPAdes[90]. Genome assemblies were assessed using QUAST for metrics, such as total contig length, GC content, N50, and N90[91]. The genomes were identified using GTDB-Tk v2.4.1 for precise taxonomic classification[92]. The draft genomes were annotated using Bakta v1.11.0[93]. Gene functions of the genomes were annotated with the Kyoto Encyclopedia of Genes and Genomes (KEGG) database using eggNOG-mapper v2.1.12[94]. Carbohydrate-active enzymes (CAZyme) were annotated using HMMER v3.4 (http://www.hmmer.org/) based on dbCAN3[95]. ARGs were searched via RGI v6.0.3 based on the comprehensive antibiotic resistance database (CARD)[96], and the VFs and virulence genes (VGs) were predicted using the VFanalyzer (https://www.mgc.ac.cn/cgi-bin/VFs/v5/main.cgi), VFs of pathogenic bacteria (VFDB)[97].

Statistics and reproducibility

The IBM SPSS Statistics software (v29.0.1.1) was used for data analysis. GraphPad Prism software (v10.1.1) was used to generate graphs. Significance analysis of lignocellulose enzyme assay was conducted across age groups and species after verifying data assumptions. Appropriate statistical tests (t-test/ANOVA or Mann-Whitney/Kruskal-Wallis) were employed for groups containing ≥5 replicates. $p < 0.05$ indicated statistically significant differences.

For strain identification, each strain was amplified using PCR three separate times and only those showing consistent results across all three replicates were selected for further study. In the lignocellulose enzyme assay, each strain was tested in three replicates, and the final enzyme activity values represent the mean of these measurements for each strain.

Reporting summary

Further information on research design is available in the Nature Portfolio Reporting Summary linked to this article.

Conclusion

In summary, this study systematically evaluated different culture conditions for *Clostridium* isolation, establishing optimized cultivation strategies that enable researchers to obtain a greater diversity of *Clostridium* isolates from the gut of GPs with less workload. Importantly, we elucidated the mechanism underlying the role of *Clostridium* in the digestion, absorption, and metabolism of nutrients from bamboo. Lignocellulose degradation capabilities were universally observed across *Clostridium* species, with substantial interspecies variability. This result provides a foundation for the screening and application of beneficial *Clostridium* isolates. However, widespread presence and dissemination of ARGs and VFs, especially in *C. perfringens*, necessitate the implementation of systematic monitoring to

assess antibiotic resistance patterns and evaluate potential pathogenic risks. Our data holds significance for understanding the complex interplay between *Clostridium* and GP health. Furthermore, the availability of isolates generated in this study enables further exploration into their potential applications in regulating the gut microbiota, alleviating gut disorders, and promoting host health.

Reporting summary

Further information on research design is available in the Nature Portfolio Reporting Summary linked to this article.

Data availability

The 16S rRNA sequencing data have been deposited in BioProject database at NCBI under accession number PRJNA1320993. The whole-genome sequencing data have been deposited in BioProject database at NCBI under accession number PRJNA1258569. All data generated or analyzed during this study are included in this published article and its supplementary files.

Received: 28 May 2025; Accepted: 24 September 2025;
Published online: 18 November 2025

References

1. Yang, S. et al. Metagenomic analysis of bacteria, fungi, bacteriophages, and helminths in the gut of giant pandas. *Front. Microbiol.* **9**, 1717–1732 (2018).
2. Liu, F. Y. et al. Age-related alterations in metabolome and microbiome provide insights in dietary transition in giant pandas. *mSystems* **8**, e0025223 (2023).
3. Yang, S. et al. Reference gene catalog and metagenome-assembled genomes from the gut microbiome reveal the microbial composition, antibiotic resistome, and adaptability of a lignocellulose diet in the giant panda. *Environ. Res.* **245**, 118090 (2023).
4. Deng, F. et al. The unique gut microbiome of giant pandas involved in protein metabolism contributes to the host's dietary adaption to bamboo. *Microbiome* **11**, 180–193 (2023).
5. Jin, L. et al. Diet, habitat environment and lifestyle conversion affect the gut microbiomes of giant pandas. *Sci. Total Environ.* **770**, 145316 (2021).
6. Huang, G. et al. PandaGUT provides new insights into bacterial diversity, function, and resistome landscapes with implications for conservation. *Microbiome* **11**, 221–235 (2023).
7. Litvak, Y., Byndloss, M. X. & Baumler, A. J. Colonocyte metabolism shapes the gut microbiota. *Science* **362**, 1017 (2018).
8. Lee, J. Y., Tsolis, R. M. & Baumler, A. J. The microbiome and gut homeostasis. *Science* **377**, eabp9960 (2022).
9. Disha, B., Flores, C., Christine, W. M. & Anna, M. S. Diversity and prevalence of *Clostridium innocuum* in the human gut microbiota. *mSphere* **8**, 00569–00522 (2023).
10. Lopetuso, L. R., Scaldaferri, F., Petito, V. & Gasbarrini, A. Commensal Clostridia: leading players in the maintenance of gut homeostasis. *Gut Pathog.* **5**, 23–30 (2013).
11. Yu, S. R. et al. *Clostridium butyricum* isolated from giant panda can attenuate dextran sodium sulfate-induced colitis in mice. *Front. Microbiol*. **15**, 1361945 (2024).
12. Zhu, L., Wu, Q., Dai, J., Zhang, S. & Wei, F. Evidence of cellulose metabolism by the giant panda gut microbiome. *PNAS* **108**, 17714–17719 (2011).
13. Prawitwong, P. et al. Direct glucose production from lignocellulose using *Clostridium thermocellum* cultures supplemented with a thermostable β-glucosidase. *Biotech. Biofuels* **6**, 184–194 (2013).
14. Silva-Andrade, C., Martin, A. J. & Garrido, D. Comparative genomics of *Clostridium baratii* reveals strain-level diversity in toxin abundance. *Microorganisms* **10**, 213–229 (2022).
15. Hassani, S., Pakbin, B., Bruck, W. M., Mahmoudi, R. & Mousavi, S. Prevalence, antibiotic resistance, toxin-typing and genotyping of *Clostridium perfringens* in raw beefmeats obtained from Qazvin City, Iran. *Antibiotics (Basel)* **11**, 340–352 (2022).
16. Li, J. et al. Toxin plasmids of *Clostridium perfringens*. *Microbiol. Mol. Biol. Rev.* **77**, 208–233 (2013).
17. Feng, Y. et al. Phylogenetic and genomic analysis reveals high genomic openness and genetic diversity of *Clostridium perfringens*. *Microb. Genom*. **6**, mgen000441 (2020).
18. Cobo, F. Antimicrobial susceptibility and clinical findings of anaerobic bacteria. *Antibiotics (Basel)* **11**, 351–353 (2022).
19. Deng, F. et al. A comprehensive analysis of antibiotic resistance genes in the giant panda gut. *Imeta* **3**, e171 (2024).
20. Feng, W. et al. Metagenome analysis reveals changes in gut microbial antibiotic resistance genes and virulence factors in reintroduced giant pandas. *Microorganisms* **13**, 1616–1618 (2025).
21. Zhao, M. Y., Li, Y. X., Wei, W., Zhang, Z. J. & Zhou, H. The distribution variation of pathogens and virulence factors in different geographical populations of giant pandas. *Front. Microbiol.* **14**, 1264786 (2023).
22. Blanco-Miguez, A. et al. Extending and improving metagenomic taxonomic profiling with uncharacterized species using MetaPhlAn 4. *Nat. Biotechnol.* **41**, 1633–1644 (2023).
23. Benoit, G. et al. High-quality metagenome assembly from long accurate reads with metaMDBG. *Nat. Biotechnol*. **42**, 1378–1383 (2024).
24. Alou, M. T. et al. State of the art in the culture of the human microbiota new interests and strategies. *Clin. Microbiol. Rev.* **34**, e00129–00119 (2021).
25. Browne, H. P. et al. Culturing of 'unculturable' human microbiota reveals novel taxa and extensive sporulation. *Nature* **533**, 543–546 (2016).
26. Lichtenegger, A. S., Posadas-Cantera, S., Badr, M. T. & Hacker, G. Comparison of the diversity of anaerobic-cultured gut bacterial communities on different culture media using 16S rDNA sequencing. *J. Microbiol. Met.* **224**, 106988 (2024).
27. Lewis, W. H., Tahon, G., Geesink, P., Sousa, D. Z. & Ettema, T. J. G. Innovations to culturing the uncultured microbial majority. *Nat. Rev. Microbiol.* **19**, 225–240 (2021).
28. Li, D. et al. The monkey microbial biobank brings previously uncultivated bioresources for nonhuman primate and human gut microbiomes. *mLife* **1**, 210–217 (2022).
29. Zou, Y. et al. 1520 reference genomes from cultivated human gut bacteria enable functional microbiome analyses. *Nat. Biotechnol.* **37**, 179–185 (2019).
30. Liu, C. et al. The mouse gut microbial biobank expands the coverage of cultured bacteria. *Nat. Commun.* **11**, 79–90 (2020).
31. Gong, R., Ye, X., Wang, S. & Ren, Z. Isolation, identification, and biological characteristics of *Clostridium sartagoforme* from rabbit. *PLoS One* **16**, e0259715 (2021).
32. Wu, K. et al. Genomic adaptation of *Clostridium perfringens* to human intestine. *iMetaOmics* **1**, e38 (2024).
33. Chai, L. J. et al. Profiling the *Clostridia* with butyrate-producing potential in the mud of Chinese liquor fermentation cellar. *Int. J. Food Microbiol.* **297**, 41–50 (2019).
34. Obiekezie, S. O., Ekeleme, I. K., Makut, M. D. & Owuna, G. Isolation, identification and production of biobutanol by different *Clostridium* species isolated from soil using waste paper and sugar cane molasses. *S. Asian J. Res. Microbiol.* **2**, 1–9 (2018).
35. Chang, Y. et al. Optimization of culturomics strategy in human fecal samples. *Front. Microbiol.* **10**, 2891–2991 (2019).
36. Lagier, J. C. et al. The rebirth of culture in microbiology through the example of culturomics to study human gut microbiota. *Clin. Microbiol. Rev.* **28**, 237–264 (2015).
37. Hou, F. et al. Application of *LpxC* enzyme inhibitor to inhibit some fast-growing bacteria in human gut bacterial culturomics. *BMC Microbiol.* **19**, 308–315 (2019).
38. Stoeva, M. K. et al. Butyrate-producing human gut symbiont, *Clostridium butyricum*, and its role in health and disease. *Gut Microbes* **13**, 1–28 (2021).

39. Hagihara, M. et al. *Clostridium butyricum* modulates the microbiome to protect intestinal barrier function in mice with antibiotic-induced dysbiosis. *iScience* **23**, 100772 (2020).
40. Huang, G. et al. Seasonal shift of the gut microbiome synchronizes host peripheral circadian rhythm for physiological adaptation to a low-fat diet in the giant panda. *Cell Rep.* **38**, 110203 (2022).
41. Du, L., Qi, R., Wang, J., Liu, Z. & Wu, Z. Indole-3-Propionic acid, a functional metabolite of *Clostridium sporogenes*, promotes muscle tissue development and reduces muscle cell inflammation. *Int. J. Mol. Sci.* **22**, 12345–12360 (2021).
42. Kiu, R. et al. Preterm Infant-Associated *Clostridium tertium*, *Clostridium cadaveris*, and *Clostridium paraputrificum* strains: genomic and evolutionary insights. *Genome Biol. Evol.* **9**, 2707–2714 (2017).
43. Munoz, M. et al. Comparative genomics identifies potential virulence factors in *Clostridium tertium* and *C. paraputrificum*. *Virulence* **10**, 657–676 (2019).
44. Grenda, T. et al. *Clostridium perfringens*—opportunistic foodborne pathogen, its diversity and epidemiological significance. *Pathogens* **12**, 768–779 (2023).
45. Duc, H. M. et al. Prevalence and antibiotic resistance profile of *Clostridium perfringens* isolated from pork and chicken meat in Vietnam. *Pathogens* **13**, 400–409 (2024).
46. AlJindan, R. et al. Genomic Insights into virulence factors and multi-drug resistance in *Clostridium perfringens* IRMC2505A. *Toxins (Basel)* **15**, 359–371 (2023).
47. Mehdizadeh Gohari, I. et al. Pathogenicity and virulence of *Clostridium perfringens*. *Virulence* **12**, 723–753 (2021).
48. Sumranwanich, T. et al. Evaluating lignin degradation under limited oxygen conditions by bacterial isolates from forest soil. *Sci. Rep.* **14**, 13350 (2024).
49. Chukwuma, O. B., Rafatullah, M., Tajarudin, H. A. & Ismail, N. A review on bacterial contribution to lignocellulose breakdown into useful bio-products. *Int. J. Environ. Res. Pub. He.* **18**, 6001–6027 (2021).
50. Jin, L. et al. Bamboo nutrients and microbiome affect gut microbiome of giant panda. *Symbiosis* **80**, 293–304 (2020).
51. Lopez-Mondejar, R., Zuhlke, D., Becher, D., Riedel, K. & Baldrian, P. Cellulose and hemicellulose decomposition by forest soil bacteria proceeds by the action of structurally variable enzymatic systems. *Sci. Rep.* **6**, 25279 (2016).
52. Li, H. et al. Accelerated degradation of cellulose in silkworm excrement by the interaction of housefly larvae and cellulose-degrading bacteria. *J. Environ. Manag.* **323**, 116295 (2022).
53. Yang, C. X., Wang, T., Gao, L. N., Yin, H. J. & Lu, X. Isolation, identification and characterization of lignin-degrading bacteria from Qinling, China. *J. Appl. Microbiol.* **123**, 1447–1460 (2017).
54. Wang, C. et al. Nutrient utilization and gut microbiota composition in giant pandas of different age groups. *Animals (Basel)* **14**, 2324–2338 (2024).
55. Wang, S. et al. Detoxification of the mycotoxin citrinin by a manganese peroxidase from *Moniliophthora roreri*. *Toxins* **14**, 801–811 (2022).
56. Diaz-Garcia, L., Bugg, T. D. H. & Jimenez, D. J. Exploring the lignin catabolism potential of soil-derived lignocellulolytic microbial consortia by a gene-centric metagenomic approach. *Microb. Ecol.* **80**, 885–896 (2020).
57. Guo, P., Zhang, K., Ma, X. & He, P. *Clostridium* species as probiotics: potentials and challenges. *J. Anim. Sci. Biotechnol.* **11**, 24–33 (2020).
58. Jobgen, W. S., Fried, S. K., Fu, W. J., Meininger, C. J. & Wu, G. Regulatory role for the arginine-nitric oxide pathway in metabolism of energy substrates. *J. Nutr. Biochem.* **17**, 571–588 (2006).
59. Stuehr, D. J. Enzymes of the L-arginine to nitric oxide pathway. *J. Nutr.* **134**, 2748S–2751 (2004).
60. Wu, G. et al. Arginine metabolism and nutrition in growth, health and disease. *Amino Acids* **37**, 153–168 (2009).
61. Jin, L. et al. Gastrointestinal microbiome, resistance genes, and risk assessment of heavy metals in wild giant pandas. *Sci. Total Environ.* **899**, 165671 (2023).
62. Wang, X. et al. Antimicrobial resistance of *Escherichia coli*, *Enterobacter spp*., *Klebsiella pneumoniae* and *Enterococcus* spp. isolated from the feces of giant panda. *BMC Microbiol* **22**, 102–112 (2022).
63. Yushchuk, O., Binda, E. & Marinelli, F. Glycopeptide antibiotic resistance genes: distribution and function in the producer Actinomycetes. *Front. Microbiol.* **11**, 1173 (2020).
64. Mustafa, G. R. et al. Metagenomic analysis revealed a wide distribution of antibiotic resistance genes and biosynthesis of antibiotics in the gut of giant pandas. *BMC Microbiol.* **21**, 15 (2021).
65. Meziane-Cherif, D. et al. Structural and functional adaptation of vancomycin resistance *Van*T serine racemases. *mBio* **6**, e00806 (2015).
66. Yim, G., Thaker, M. N., Koteva, K. & Wright, G. Glycopeptide antibiotic biosynthesis. *J. Antibiotics (Tokyo)* **67**, 31–41 (2014).
67. Hu, T. et al. Geographic pattern of antibiotic resistance genes in the metagenomes of the giant panda. *Microb. Biotechnol.* **14**, 186–197 (2021).
68. Yan, Z. et al. The impact of bamboo consumption on the spread of antibiotic resistance genes in giant pandas. *Vet. Sci.* **10**, 630–643 (2023).
69. Yan, Z. et al. Dietary microbiota-mediated shifts in gut microbial ecology and pathogen interactions in giant pandas (*Ailuropoda melanoleuca*). *Commun. Biol.* **8**, 864–877 (2025).
70. Fu, Y. et al. Co-occurrence patterns of gut microbiome, antibiotic resistome and the perturbation of dietary uptake in captive giant pandas. *J. Hazard. Mater.* **471**, 134252 (2024).
71. Deng, W. W. et al. Heavy metals, antibiotics and nutrients affect the bacterial community and resistance genes in chicken manure composting and fertilized soil. *J. Environ. Manag.* **257**, 109980 (2020).
72. Yan, M. et al. Emerging antibiotic and heavy metal resistance in spore-forming bacteria from pig manure, manure slurry and fertilized soil. *J. Environ. Manag.* **371**, 123270 (2024).
73. Dong, W. et al. An expanded database and analytical toolkit for identifying bacterial virulence factors and their associations with chronic diseases. *Nat. Commun.* **15**, 8084–8099 (2024).
74. Yang, Q. et al. Evaluation of immunogenicity and protective efficacy of the elongation factor Tu against *Streptococcus agalactiae* in tilapia. *Aquaculture* **492**, 184–189 (2018).
75. Harvey, K. L., Jarocki, V. M., Charles, I. G. & Djordjevic, S. P. The diverse functional roles of elongation factor Tu (EF-Tu) in microbial pathogenesis. *Front. Microbiol.* **10**, 2351–2369 (2019).
76. Muscariello, L., De Siena, B. & Marasco, R. Lactobacillus cell surface proteins involved in interaction with mucus and extracellular matrix components. *Curr. Microbiol.* **77**, 3831–3841 (2020).
77. Wuppermann, F. N., Molleken, K., Julien, M., Jantos, C. A. & Hegemann, J. H. Chlamydia pneumoniae GroEL1 protein is cell surface associated and required for infection of HEp-2 cells. *J. Bacteriol.* **190**, 3757–3767 (2008).
78. Hennequin, C. et al. GroEL (Hsp60) of *Clostridium difficile* is involved in cell adherence. *Microbiology (Reading)* **147**, 87–96 (2001).
79. Zhu, D. et al. Characterization of molecular chaperone *GroEL* as a potential virulence factor in *Cronobacter sakazakii*. *Foods* **12**, 3404–3419 (2023).
80. Melville, S. & Craig, L. Type IV pili in Gram-positive bacteria. *Microbiol. Mol. Biol. Rev.* **77**, 323–341 (2013).
81. Kiu, R., Caim, S., Alexander, S., Pachori, P. & Hall, L. J. Probing genomic aspects of the multi-host pathogen *Clostridium perfringens* reveals significant pangenome diversity, and a diverse array of virulence factors. *Front. Microbiol.* **8**, 2485–2502 (2017).
82. Rood, J. I. et al. Expansion of the *Clostridium perfringens* toxin-based typing scheme. *Anaerobe* **53**, 5–10 (2018).
83. Camargo, A. et al. Intra-species diversity of *Clostridium perfringens*: A diverse genetic repertoire reveals its pathogenic potential. *Front. Microbiol.* **13**, 952081 (2022).

84. Kiu, R. et al. Particular genomic and virulence traits associated with preterm infant-derived toxigenic *Clostridium perfringens* strains. *Nat. Microbiol.* **8**, 1160–1175 (2023).
85. Hafner, L. et al. Differential stress responsiveness determines intraspecies virulence heterogeneity and host adaptation in *Listeria monocytogenes*. *Nat. Microbiol.* **9**, 3345–3361 (2024).
86. Forti, K. et al. Molecular characterization of *Clostridium perfringens* strains isolated in Italy. *Toxins (Basel)* **12**, 650–669 (2020).
87. Chang, Y. X., Hou, F. Y., Bi, Y. J. & Yang, R. F. Optimization of culturomics methods. *Microbiome Protoc. ebook* **Bio-101**, e2003639 (2021).
88. Sharker, B. et al. Characterization of lignin and hemicellulose degrading bacteria isolated from cow rumen and forest soil: unveiling a novel enzymatic model for rice straw deconstruction. *Sci. Total Environ.* **904**, 166704 (2023).
89. Haque, M. A. et al. Rapid deconstruction of cotton, coir, areca, and banana fibers recalcitrant structure using a bacterial consortium with enhanced saccharification. *Waste Biomass-. Valor.* **12**, 4001–4018 (2020).
90. Bankevich, A. et al. SPAdes: a new genome assembly algorithm and its applications to single-cell sequencing. *J. Comput. Biol.* **19**, 455–477 (2012).
91. Gurevich, A., Saveliev, V., Vyahhi, N. & Tesler, G. QUAST: quality assessment tool for genome assemblies. *Bioinformatics* **29**, 1072–1075 (2013).
92. Chaumeil, P. A., Mussig, A. J., Hugenholtz, P. & Parks, D. H. GTDB-Tk v2: memory friendly classification with the genome taxonomy database. *Bioinformatics* **38**, 5315–5316 (2022).
93. Schwengers, O. et al. Bakta: rapid and standardized annotation of bacterial genomes via alignment-free sequence identification. *Microb. Genom.* **7**, 000685 (2021).
94. Cantalapiedra, C. P., Hernandez-Plaza, A., Letunic, I., Bork, P. & Huerta-Cepas, J. eggNOG-mapper v2: functional annotation, orthology assignments, and domain prediction at the metagenomic scale. *Mol. Biol. Evol.* **38**, 5825–5829 (2021).
95. Zheng, J. et al. dbCAN3: automated carbohydrate-active enzyme and substrate annotation. *Nucleic Acids Res.* **51**, W115–W121 (2023).
96. Jia, B. et al. CARD 2017: expansion and model-centric curation of the comprehensive antibiotic resistance database. *Nucleic Acids Res.* **45**, D566–D573 (2017).
97. Liu, B., Zheng, D., Jin, Q., Chen, L. & Yang, J. VFDB 2019: a comparative pathogenomic platform with an interactive web interface. *Nucleic Acids Res.* **47**, D687–D692 (2019).

Acknowledgements

This work was supported by the International Cooperation Funding Project for Giant Pandas (The Giant Panda Microbiome Research and Biobank Establishment).

Author contributions

L. Zou, K. Zhao, and C. Li contributed to the design of this study and revised the manuscript. Y. Huang and D. Li contributed to supervising this study. W. Deng and C. Liu performed the experiment and collected data. W. Deng, and S. Yang performed data analysis and drafted the manuscript. T. Li and D. Wu contributed to sample collection. Y. He and R. Li conducted scientific direction and provided valuable comments. All authors reviewed and agreed to the final version of the manuscript.

Competing interests

The authors declare no competing interests.

Additional information

Supplementary information The online version contains supplementary material available at https://doi.org/10.1038/s42003-025-08943-7.

Correspondence and requests for materials should be addressed to Shengzhi Yang, Likou Zou or Ke Zhao.

Peer review information *Communications Biology* thanks Francesco Candeliere and Lei Wang for their contribution to the peer review of this work. Primary Handling Editors: Sabina La Rosa and Tobias Goris. A peer review file is available.

Reprints and permissions information is available at http://www.nature.com/reprints

Publisher's note Springer Nature remains neutral with regard to jurisdictional claims in published maps and institutional affiliations.

Open Access This article is licensed under a Creative Commons Attribution-NonCommercial-NoDerivatives 4.0 International License, which permits any non-commercial use, sharing, distribution and reproduction in any medium or format, as long as you give appropriate credit to the original author(s) and the source, provide a link to the Creative Commons licence, and indicate if you modified the licensed material. You do not have permission under this licence to share adapted material derived from this article or parts of it. The images or other third party material in this article are included in the article's Creative Commons licence, unless indicated otherwise in a credit line to the material. If material is not included in the article's Creative Commons licence and your intended use is not permitted by statutory regulation or exceeds the permitted use, you will need to obtain permission directly from the copyright holder. To view a copy of this licence, visit http://creativecommons.org/licenses/by-nc-nd/4.0/.

© The Author(s) 2025